INORGANIC CHEMISTRY

FRONTIERS

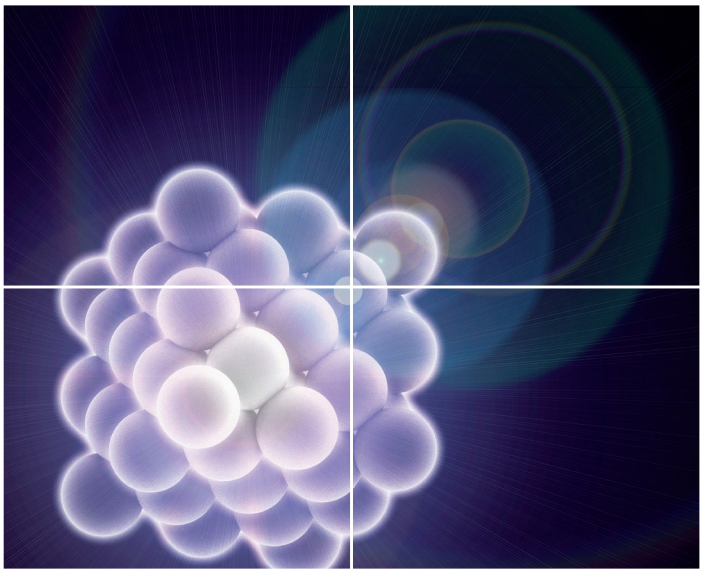

Accepted Manuscript

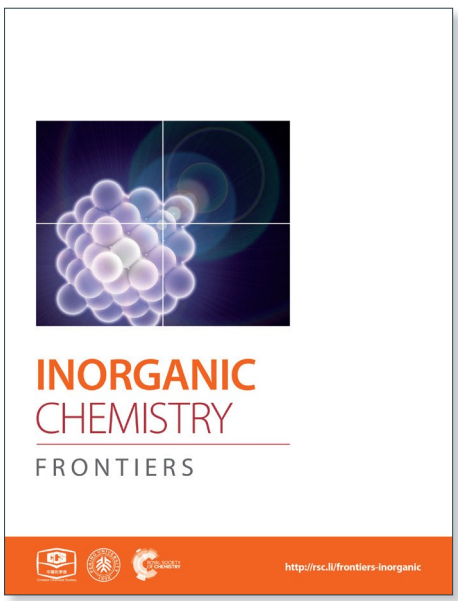

This is an *Accepted Manuscript*, which has been through the Royal Society of Chemistry peer review process and has been accepted for publication.

Accepted Manuscripts are published online shortly after acceptance, before technical editing, formatting and proof reading. Using this free service, authors can make their results available to the community, in citable form, before we publish the edited article. We will replace this *Accepted Manuscript* with the edited and formatted *Advance Article* as soon as it is available.

You can find more information about *Accepted Manuscripts* in the **Information for Authors**.

Please note that technical editing may introduce minor changes to the text and/or graphics, which may alter content. The journal's standard **Terms & Conditions** and the **Ethical guidelines** still apply. In no event shall the Royal Society of Chemistry be held responsible for any errors or omissions in this *Accepted Manuscript* or any consequences arising from the use of any information it contains.

Journal Name

ARTICLE

Recent Developments in the Catalytic Hydrogenation of CO_2 to Formic acid/Formate using Heterogeneous Catalysts

maReceived 00th January 20xx,
Accepted 00th January 20xx

DOI: 10.1039/x0xx00000x

www.rsc.org/

Gunniya Hariyanandam Gunasekar,[a†] Kwangho Park,[a†] Kwang-Deog Jung[b] and Sungho Yoon[a]

The conversion of CO_2 into value added chemicals is one of the fascinating strategies to mitigate the level of CO_2 in the atmosphere. Specifically, the hydrogenation of CO_2 into formic acid/formate has received a great deal of attention since the product is a valuable basic chemical as well as a promising energy storage material. However due to the kinetic and thermodynamic limitations of this conversion, developing an efficient catalytic system has become desirable. Therefore various approaches have been implemented for the development of both homogeneous and heterogeneous catalysts. In this context, the recent advances in the hydrogenation of CO_2 to formic acid/formate using heterogeneous catalysts as well as theoretical investigations are presented.

[a] Department of Bio&Nano Chemistry
Kookmin University
861-1 Jeongneung-dong, Seongbuk-gu, Republic of Korea
E-mail: yoona@kookmin.ac.kr
[b] Clean Energy Research Centre
Korea Institute of Science and Technology
P.O. Box 131, Cheongryang, Seoul 136-791, Republic of Korea
† These authors contributed equally to this work

1. Introduction

In recent years, climate change and increasing global temperatures due to the anthropogenic emission of CO_2 into the atmosphere have caused increasing concern. The concentration of CO_2 in the atmosphere has reached unprecedented levels (~400 ppm), mainly due to the utilization of carbon-rich fossil fuels, such as coal, oil and natural gas.[1-2] Thus, reducing the emission of CO_2, utilizing the abundant CO_2 in the atmosphere and recycling CO_2 have attracted much attention.[3-6] Recently, "Lima call for climate action" targeted a near-zero anthropogenic emission of CO_2 by the end of the century, highlighting the concern over atmospheric CO_2 levels.[7-8] Consequently, research into renewable fuels, CO_2 storage and CO_2 utilization has gained increased attention in the scientific and technological community.[9-12]

CO_2 is emerging as an attractive C1 feedstock for producing various chemicals owing to the fact that it is safe, abundant, nontoxic, economical and renewable. Such CO_2-based products are not only profitable, but are also alternatives to those derived from petroleum resources, and could therefore lessen petroleum dependence in society.[13-17] However, very few industrial processes, largely limited to those involving urea, salicylic acid and carbonate synthesis, utilize CO_2 as a raw material.[18]

One important chemical, out of diverse chemical products derived based on CO_2 as a C1 feedstock, is formic acid, which is a valuable basic chemical used as preservative, antibacterial agent, insecticide and also as de-icing agent in various

Gunniya Hariyanandam Gunasekar

Gunniya Hariyanandam Gunasekar received his Master's degree in Chemistry from Madurai Kamaraj University, India in the year of 2009. He has worked as a research executive in Orchid Chemicals and Pharmaceuticals R & D Centre during 2009-2013. Currently, he is pursuing his Ph.D. degree in the group of Prof. Sungho Yoon at Kookmin University, South Korea. His research interests focus on the transformations of CO_2 as well as the development of multifunctional COF materials.

Kwangho Park

Kwangho Park obtained his B.S. degree in Chemistry at the Department of Bio and Nano chemistry from Kookmin University in 2014. Currently, he is a Master's degree student in Kookmin University, working in the Nano Inorganic Lab under Prof. Sungho Yoon. His research interests include CO_2 capture, CO_2 hydrogenation and the development of covalent triazine framework materials.

industries.[19-20] In addition, it plays a major role in the synthetic chemistry as an acid, a reductant and a precursor for syntheses. Moreover, it is being considered as a hydrogen storage material in energy industries. Even though formic acid has a relatively low H_2 content (4.4 wt%), it is easy to store and transport.[21] Recently, formic acid has emerged as a promising fuel source in direct liquid fuel cell systems due to its excellent oxidation kinetics, high cell potential and less fuel crossover problems.[22] Thus, the myriad applications of formic acid as well as CO_2 utilization attracts the hydrogenation of CO_2 to formic acid/formates in the scientific and technological community to a greater extent.

Currently 800,000 T of formic acid is produced per year in the industries using toxic carbon monoxide and methanol.[23] According to Barcow and coworker's, this process could emit ca. 3076 kg of CO_2 for the production of 1 T of formic acid, whereas only 100 kg of CO_2 could be emitted, if the same is produced by CO_2 hydrogenation process.[24] Hence, CO_2-based production has enormous potential to reduce the environmental impact when compared with conventional CO-based method.

The hydrogenation of CO_2 to formic acid involves the conversion of gases substances into liquid products and hence the reaction is entropically disfavored. Thus, the reaction is endergonic in the gas phase (ΔG°_{298} = 32.9 kJ mol^{-1}) and is exergonic in the aqueous (solvation) phase (ΔG°_{298} = -9.5 kJ mol^{-1}). In addition, the equilibrium can be shifted towards the product side using certain bases, such as ammonia (NH_3) and triethylamine (NEt_3) (eqs. 1-3).[25] Moreover, the chemical equilibrium of CO_2/bicarbonate (HCO_3^-)/carbonate (CO_3^{2-}) is influenced by many parameters, such as temperature, CO_2 pressure, kind of base, and solution pH. Thus, the actual form of the substrate in this reaction is ambiguous. Henceforth, the term 'hydrogenation of CO_2' being used in this review and elsewhere may actually involve HCO_3^-/CO_3^{2-} as the real substrate.

Since the discovery of phosphine-based Ru complexes by Inoue *et al.*,[26] excellent progress has been achieved in the development of homogeneous catalysts.[27-32] In particular, extensive studies on homogeneous Ir, Ru, and Rh complexes have been reported, and recently, half-sandwich Ir derivatives and Ru/Ir-pincer complexes have shown tremendous catalytic activities, with a maximum turnover number (TON) of 3,500,000 and a maximum turnover frequency (TOF) of 1,100,000 h^{-1}.[33-40]

Despite the homogeneous catalysts exhibiting excellent catalytic efficiencies for the hydrogenation of CO_2 to formate, industries are reluctant to use them for large-scale production, owing to the difficulty in catalyst separation from the final reaction mixture.[41] Importantly, these homogeneous catalysts also promotes the decomposition of generated formate back into CO_2 and H_2 during the product separation step(s).[23,42-43] Because of such limitations, diverse heterogeneous catalysts which have strong merit in separation were reported.

While many reviews and books have been focused on CO_2 hydrogenation to formate using homogeneous catalysts,[44-47] summarization of heterogeneous catalysts on CO_2 hydrogenation are not available yet. Therefore, for the first time, the progress that has been achieved in the development of heterogeneous catalysts for this conversion is presented here. In order to explore the prospective design for highly active and industrially viable heterogeneous catalysts we have segmented this review based on the type of catalysts and the catalyst supports employed. The organization of this review is as follows; it has categorized into three major sections excluding introduction and conclusion. After this introduction, the second section provides the application of heterogeneous metal catalysts. This section is subdivided into two parts based on the type of metal catalysts employed: section 2.1 explores the performances of bulk metal catalysts; section 2.2 presents the catalytic efficiencies of supported metal catalysts. The third section addresses the application of heterogenized molecular catalysts. This section is further classified into two parts based on the kind of heterogenization processes followed; section 3.1 deal with the efficiencies of metal complexes heterogenized by grafting methods; section 3.2 explores the performances of metal complexes heterogenized by incorporating into the support's pore wall. Since

Kwang-Deog Jung

Dr Kwang-Deog Jung received his bachelor's degree and Ph.D. in Chemical Engineering from Yonsei University in 1985 and Korea Advanced Institute of Science and Technology in 1996, respectively. He has worked on C1 chemistry and processes in Korea Institute of Science and Technology since 1997. His research interests focus on the synthesis of heterogeneous catalysts and the catalytic processes for hydrogenation of CO and CO_2, hydrogen production, carbonylation of CO and electrochemical CO_2 reduction.

Sungho Yoon

Prof. Sungho Yoon received his B.S. and Ph.D. degree from Korea University in 1998 and Massachusetts Institute of Technology in 2004, respectively, and worked as a post-doctoral fellow at University of California, Berkeley during 2004-2005 and a researcher at LG Chem. Research Park during 2005-2007. He has worked on C1 chemistry in Kookmin University since 2007. His research interests focus on the synthesis of covalent organic frameworks and catalysts for hydrogenation and carbonylation.

	ΔG° (kJ mol^{-1})	ΔH° (kJ mol^{-1})	ΔS° (J mol^{-1} K^{-1})	
$CO_2(g) + H_2(g) \rightleftharpoons HCO_2H(l)$	32.9	-31.2	-216	(1)
$CO_2(g) + H_2(g) + NH_3(aq) \rightleftharpoons HCO_2^-(aq) + NH_4^+(aq)$	-9.5	-84.3	-250	(2)
$CO_2(aq) + H_2(aq) + NH_3(aq) \rightleftharpoons HCO_2^-(aq) + NH_4^+(aq)$	-35.4	-59.8	-81	(3)

covalent organic framework (COF) based supports have only been utilized in the literature, we entitled this section as "Heterogenized COFs catalyst". The section four briefly explores the theoretical investigations on this topic and in the final section, we briefly summarized the status and perspectives of this field.

2. Heterogeneous Metal Catalysts

2.1 Bulk Metal Catalysts

The research on hydrogenation of CO_2 to formate began in 1935 by Adkins *et al.* using RANEY® nickel (Ra-Ni) catalyst and they reported 57 % yield at 80-150 ˚C under high pressure (20-40 MPa) in Ethanol (EtOH)/Phenol solvent system (Table 1, entry 1).[48] Even though the reaction was not catalytic (TON <1), it initiated a new field of research which is the conversion of relatively cheap and abundant CO_2 into value added chemicals. After a while, Stalder *et al.* employed Pd black as a catalyst for the conversion (entry 2) and observed catalytic conversion (TON 2.1) in 1 M aqueous $NaHCO_3$ solution after long reaction times (53 h).[49] Takahashi *et al.* used a mixture of Fe and Ni powder as a catalyst under hydrothermal conditions (300 ˚C) using water (H_2O) as a hydrogen source; however, the yield of formate was very low (TON 0.022).[50] Later, Fachinetti *et al.* broadened their search to Group 8-11 metal blacks.[51] Initially they screened metals that promote the reverse reaction that is decomposition of formate salts to CO_2 and H_2, as they necessarily promote the hydrogenation of CO_2 to formate. Transition metals (Group 8-11), such as Fe, Co, Ni, Cu, Ru, Rh, Pd, Ag, Ir, Pt and Au were screened for the decomposition of formic acid-NEt_3 ($HCOOH/NEt_3$) adducts to CO_2 and H_2 at 40 ˚C, and only Au metal blacks showed gas evolution, indicating that only Au metal had the potential to promote the hydrogenation of CO_2 to formate. Since then, Au black was examined as a catalyst for the hydrogenation of CO_2 to formate at 40 ˚C in NEt_3 solution, and the results showed that Au black fairly converted CO_2 to formate. However, deactivation of the catalyst was observed during the reaction, which was due to the aggregation of catalytic metal particles during the reaction, leading to the number of active sites on the surface of the catalyst being reduced. This result clearly explains the low catalytic efficiencies of bulk metals and also the inevitability of a support to stabilize metal blacks.

2.2 Supported Metal Catalysts

Since heterogeneous catalytic reactions are surface reactions, they typically follow the following steps: (1) the adsorption of reactants onto the surface of the catalyst; (2) surface reaction of adsorbed reactants with the catalyst; and (3) desorption of products from the surface of the catalyst.[52] Since the number of metal atoms on the surface of a bulk metal is extremely small compared to the number of metal atoms in the interior, a large number of active metal atoms are not exposed to the reactants, which makes bulk metals economically inefficient to use in catalytic processes. Moreover, as these bulk metals often aggregate under reaction conditions, the number of active metal atoms on the surface of the catalyst is reduced further. To overcome these problems, catalytically active metals are often dispersed on solid supports.

Since the Au blacks aggregated under reaction conditions, Fachinetti *et al.* employed titanium dioxide (TiO_2) supported Au particles (1 wt% Au) for this conversion.[51] The supported Au particles (AUROlite®) showed superior catalytic conversion than unsupported Au particles, and attained a TON of 855 at 40 ˚C under 18 MPa total pressure in NEt_3 solution for 3 days (entry 3). Importantly, 1.3 kg of $HCOOH/NEt_3$ adduct with an acid to amine ratio of 1.7 was obtained after 37 days of continuous production. This result showed that, unlike bulk Au black, the supported Au particles were very stable during the reaction conditions. However, owing to the Au-catalyzed reverse water gas shift reaction, the accumulation of CO (63 mmol) was observed, which consequently slowed the reaction.[53]

Recently Pidko and co-workers employed both supported and unsupported Au nanoparticles [Au NP(s)] as a catalyst for this reaction.[54] They also observed the superior catalytic efficiency of supported Au NPs than unsupported Au NPs. They employed a series of supports namely, Al_2O_3, TiO_2, ZnO, CeO_2, MgAl-HT (hydrotalcite), MgCr-HT and $CuCr_2O_4$, to stabilize the Au NPs and studied their catalytic efficiencies (entries 4-10). Of the various supports employed, the Au NP supported on Al_2O_3 (Au NP/Al_2O_3) has showed better catalytic performance (TON 215) (entry 4). Notably, Au NP/Al_2O_3 exhibited a twofold higher catalytic efficiency than the titania-supported Au NP (Au NP/TiO_2) (entries 4 and 5). This superior performance of Au NP/Al_2O_3 is believed to be the synergetic effect of Au NPs and Al_2O_3 support. The temperature dependent TOF values and the kinetic modeling results revealed that the Au NP/Al_2O_3 has a near-zero apparent activation energy (1.2 kcal mol^{-1}). Based on the spectroscopic data and previous studies, they proposed a plausible mechanism in which the Au-H species, formed from the heterolytic dissociation of H_2, react with the surface bicarbonate species and form Au-formate intermediate. This surface formate species would migrate to the more stable alumina surface and subsequently formates are released from the catalytic cycle.

Previously, Stalder *et al.* studied the catalytic efficiency of a series of supported Pd species for the conversion of $NaHCO_3$ to formate under ca. 0.1 MPa H_2 pressure.[49] Three types of

Table 1. Comparison of catalytic systems for the hydrogenation of CO_2 to formic acid/formate

Entry	Catalyst	Temperature (˚C)	$p(H_2)/p(CO_2)$ (MPa)	Solvent	Additive/ base	Time (h)	TON/Final formate concentration (M)	TOF (h^{-1})	Ref
1	Ra-Ni	100	4-14/6	EtOH/ Phenol	2,2,6,6-Tetra-Me-4-OH piperidine	6	-/0.31	<1	48
2	Pd black	25	0.1/0	H_2O	$NaHCO_3$	53	2.1/0.19	<1	49
3	AUROlite®	40	9/9	NEt_3	NEt_3	52	855	16.4	51
4	Au NP/Al_2O_3	70	20/20	EtOH	NEt_3	20	215/0.20	11	53
5	Au NP/TiO_2	70	20/20	EtOH	NEt_3	20	111/0.09	5.5	54
6	Au NP/ZnO	70	20/20	EtOH	NEt_3	20	2/<0.01	<1	54
7	Au NP/CeO_2	70	20/20	EtOH	NEt_3	20	8/<0.01	<1	54
8	Au NP/MgAl-HT	70	20/20	EtOH	NEt_3	20	91/0.01	4.5	54
9	Au NP/MgCr-HT	70	20/20	EtOH	NEt_3	20	52/<0.01	2.6	54
10	Au NP/$CuCr_2O_4$	70	20/20	EtOH	NEt_3	20	6/<0.01	<1	54
11	Pd/$BaSO_4$	25	0.1/0	H_2O	$NaHCO_3$	50	19/0.09	<1	49
12	Pd/γ- Al_2O_3	25	0.1/0	H_2O	$NaHCO_3$	53	50/0.23	<1	49
13	Pd/C	25	0.17/0	H_2O	$NaHCO_3$	46	115/0.54	2.5	49
14	Pd/AC	20	2.75/0	H_2O	$NaHCO_3$	1	527/0.28	527	55
15	Pd/AC	20	2.75/0	H_2O	$KHCO_3$	1	567/0.30	567	55
16	Pd/AC	20	2.75/0	H_2O	NH_4HCO_3	1	782/0.42	782	55
17	Pd/AC	20	2.75/0	H_2O	Na_2CO_3	1	<1/<0.01	<1	55
18	Pd/AC	20	2.75/0	H_2O	K_2CO_3	1	<1/<0.01	<1	55
19	Pd/AC	20	2.75/0	H_2O	$(NH_4)_2CO_3$	1	278/0.15	278	55
20	Pd/AC	20	2.75/0	H_2O	NH_4HCO_3	15	1769/0.95	118	55
21	Pd/AC	20	5.52/0	H_2O	NH_4HCO_3	2	1672/0.90	836	55
22	Pd/Al_2O_3	20	2.75/0	H_2O	NH_4HCO_3	1	278/0.08	278	55
23	Pd/$CaCo_3$	20	2.75/0	H_2O	NH_4HCO_3	1	20/<0.01	20	55
24	Pd/$BaSO_4$	20	2.75/0	H_2O	NH_4HCO_3	1	212/0.02	212	55
25	Pd/AC	20	2.75/0	EtOH/ H_2O (7/3)	$NH_2CO_2NH_4$	8	845/0.91	105	56
26	Pd/r-GO (1 wt%)	100	4/0	H_2O	$KHCO_3$	32	7088/4.53	221	57
27	Pd/r-GO (2 wt%)	100	4/0	H_2O	$KHCO_3$	10	2117/4.06	211	57
28	Pd/r-GO (5 wt%)	100	4/0	H_2O	$KHCO_3$	10	1658/3.18	165	57
29	PdNi/CNT-GR	40	25/25	H_2O	nil	15	6.4/0.02	<1	58
30	Ru/MgO	80	5/8.5	EtOH	NEt_3	1	0	-	58
31	Ru/AC	80	5/8.5	EtOH	NEt_3	1	10/0.05	10	58
32	Ru/γ-Al_2O_3	80	5/8.5	EtOH	NEt_3	1	91/0.455	91	58

Entry	Catalyst	Temperature (˚C)	$p(H_2)/p(CO_2)$ (MPa)	Solvent	Additive/ base	Time (h)	TON/Final formate concentration (M)	TOF (h^{-1})	Ref
33	Ru/γ-Al_2O_3(n))	80	5/8.5	EtOH	NEt_3	1	731/0.68	731	60
34	**3**	80	5.4/9.3	EtOH	PPh_3/NEt_3	1	1022/0.40	1022	62
35	**4**	80	4/12	EtOH	PPh_3/NEt_3	1	656/0.52	656	63
36	**5**	80	5/8	EtOH	PPh_3/NEt_3	1	151/0.36	151	65
37	**6**	80	5.4/9.3	EtOH	PPh_3/NEt_3	1	723/0.28	723	66
38	**7**	80	5.4/9.3	EtOH	PPh_3/NEt_3	1	537/0.21	537	66
39	**8**	80	4/12	EtOH	PPh_3/NEt_3	1	1384/1.10	1384	63
40	**9**	80	4/12	EtOH	PPh_3/NEt_3	1	868/0.69	868	63
41	**10**	80	5/8	EtOH	PPh_3/NEt_3	1	75/0.18	75	65
42	**11**	80	5/8	EtOH	PPh_3/NEt_3	1	143/0.34	143	65
43	**5**	80	5/8	EtOH	dppe/NEt_3	1	191/0.45	191	65
44	**5**	80	5/8	EtOH	$AsPh_3/NEt_3$	1	29/0.06	29	65
45	**3**	80	5.4/9.3	EtOH	NPh_3/NEt_3	1	179/0.07	179	66
46	**3**	80	5.4/9.3	EtOH	$AsPh_3/NEt_3$	1	171/0.06	171	66
47	**12**	60	2/2	H_2O	NEt_3	2	1300/0.13	620	70
48	**13**	60	2/2	H_2O	NEt_3	2	110/0.01	55	70
49	**14**	60	2/2	H_2O	NEt_3	2	400/0.04	200	70
50	**15**	60	2/2	H_2O	NEt_3	1	0	0	70
51	**16**	60	2/2	H_2O	NEt_3	2	70/<0.01	35	70
52	**12**	60	2/2	H_2O	NEt_3	1	880/0.08	880	70
53	**12**	90	2/2	H_2O	NEt_3	1	1100/0.11	1100	70
54	**12**	120	2/2	H_2O	NEt_3	2	2300/0.23	1200	70
55	**12**	60	2/2	H_2O	NEt_3	20	2700/0.27	140	70
56	**17**	120	2/2	H_2O	NEt_3	1	248/0.04	248	71
57	**18**	120	2/2	H_2O	NEt_3	1	38/<0.01	38	71
58	**19**	120	2/2	H_2O	NEt_3	1	132/0.02	132	71
59	**20**	40	6/6	NEt_3	NEt_3	24	25	1	79
60	**20**	60	6/6	NEt_3	PPh_3	24	2254	94	79
61	**21**	150	2/2	D_2O	NEt_3	24	81/0.28	3.3	80
62	**21**	150	2.7/1.3	D_2O	NEt_3	24	106/0.37	4.4	80
63	**21**	150	3/1	D_2O	NEt_3	24	95/0.34	3.9	80
64	**21**	150	3.5/0.5	D_2O	NEt_3	24	77/0.27	3.2	80
65	**23**	80	2/2	H_2O	NEt_3	2	500/0.06	250	81
66	**23**	120	2/2	H_2O	NEt_3	2	3320/0.40	1660	81
67	**23**	160	2/2	H_2O	NEt_3	2	2700/0.33	1350	81
68	**23**	200	2/2	H_2O	NEt_3	2	1320/0.16	660	81
69	**23**	120	4/4	H_2O	NEt_3	2	5000/0.61	2500	81
70	**23**	120	4/4	H_2O	NEt_3	0.25	1300/0.15	5300	81

Entry	Catalyst	Temperature (˚C)	$p(H_2)/p(CO_2)$ (MPa)	Solvent	Additive/ base	Time (h)	TON/Final formate concentration (M)	TOF (h^{-1})	Ref
71	**25**	120	4/4	H_2O	NEt_3	0.5	750/0.01	1500	82
72	**25**	120	4/4	H_2O	NEt_3	10	6400/0.14	640	82

supports, namely $BaSO_4$, γ-Al_2O_3 and carbon were employed, and all the supported Pd catalysts (Pd/$BaSO_4$, Pd/γ-Al_2O_3 and Pd/C) showed better activity than unsupported Pd black under similar reaction conditions, again revealing the importance of catalyst supports (entries 2, 11-13). Among the supported catalysts, Pd/C showed the maximum TON (115) at 25 ˚C (entries 11-13). Additionally, Ni, Ru, Rh and Pt metals supported on γ-Al_2O_3 also catalyzed the reaction, but to a lesser extent than Pd.

Recently, Su *et al.* employed a porous carbon material (activated carbon) as a support (Pd/AC) and systematically studied the conversion of various bicarbonate salts to formates under relatively high H_2 pressures (0.69-5.52 MPa).[55] The Pd/AC showed a higher TOF (527 h^{-1}) than the Pd/C (TOF 2.5 h^{-1}), indicating the benefit of porous catalyst supports for the reaction (entries 13 and 14). In addition, various carbonates (Na_2CO_3, K_2CO_3 and $(NH_4)_2CO_3$) and bicarbonates ($NaHCO_3$, $KHCO_3$ and NH_4HCO_3) were screened and it was found that the hydrogenation of carbonate salts was much more difficult than the bicarbonate salts (entries 14-19). This is because the protonation of carbonate ions was the rate limiting step at this temperature. Of the bicarbonate salts screened, NH_4HCO_3 gave higher yield (42.4 %, TON 782) than $NaHCO_3$ (28.6 %, TON 527) and $KHCO_3$ (30.8 %, TON 567) (entries 14-16). The high yield of formate from NH_4HCO_3 salt was thought to be caused by higher equilibrium concentration of HCO_3^- ions (0.92 M) over CO_3^{2-} ions than that of $KHCO_3$ (0.89 M) or $NaHCO_3$ salts (0.61 M).

However, the yield of formate was decreased at higher temperatures because Pd/AC promoted the decomposition of

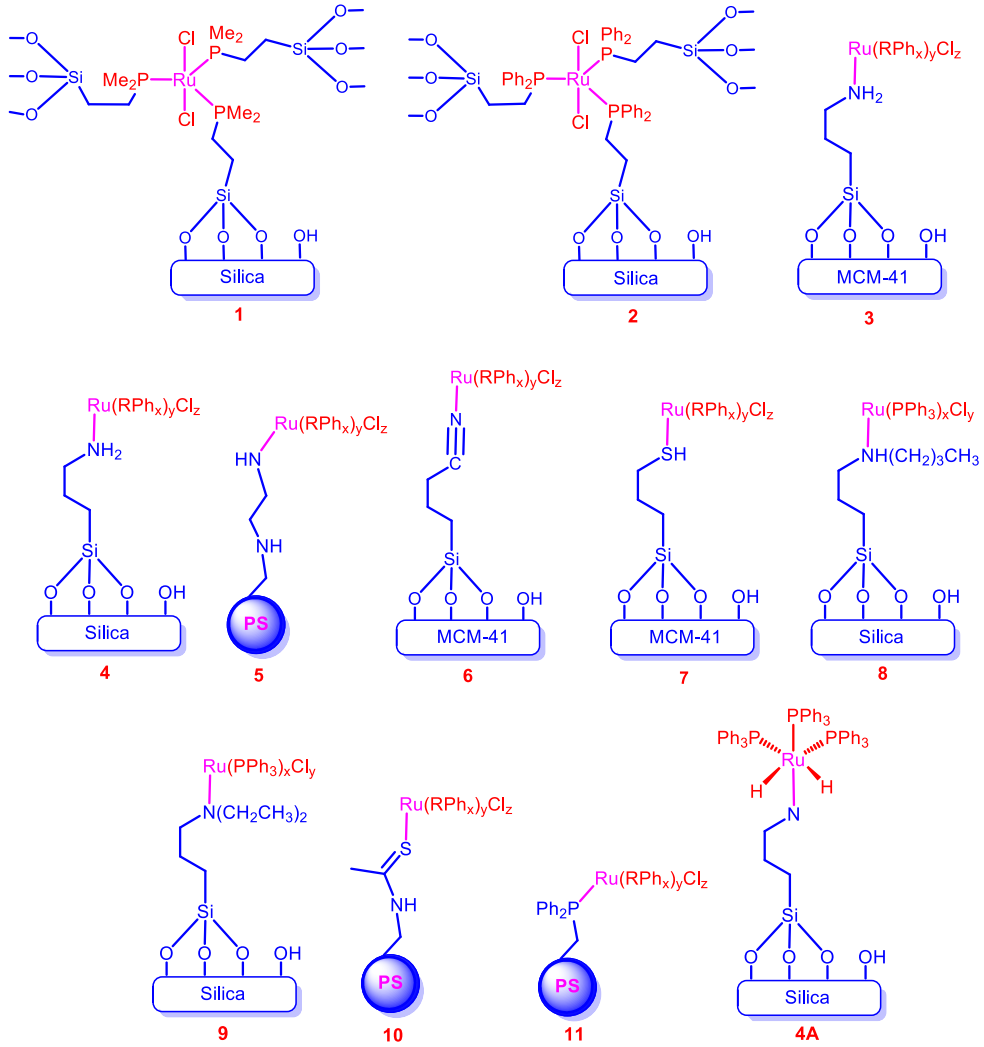

Chart 1. Representative structures of catalysts **1-11**

ammonium formate back into CO_2, H_2 and NH_3 to a large extent at higher temperatures. Therefore, maximum activity was obtained at high H_2 pressure (5.52 MPa) and long reaction time (entries 20 and 21). In addition, various catalyst supports ($BaSO_4$, $CaCO_3$ and γ-Al_2O_3) were also screened and it was found that Pd/AC exhibited better catalytic performance than the others (entries 16, 22-24). This was attributed to the hydrophobic nature of activated carbon, which results in the accumulation of H_2 on the surface of the support. In addition to the above salts ($NaHCO_3$, $KHCO_3$ and NH_4HCO_3), ammonium carbamate salt ($NH_2CO_2NH_4$) was also studied.[56] It was shown that the activities of these salts were depend on the solvents employed. For example, in pure H_2O solution, $NaHCO_3$ (0.5 M) showed the maximum yield of 23 % but in pure EtOH solution, $NH_2CO_2NH_4$ (0.5 M) exhibited the maximum yield of 40 %. The yield of $NH_2CO_2NH_4$ was improved to 44 % in EtOH-H_2O mixture (7:3), and it was expected due to the formation of ethyl carbamate salt in the EtOH-H_2O mixture. The Pd/AC showed the maximum TON of 845 using $NH_2CO_2NH_4$ salt at 20 ˚C under 2.75 MPa H_2 pressure (entry 25). Furthermore, the catalytic efficiency of Pd/AC was maintained over repeated recycling.

Yong Cao and co-workers evaluated the catalytic performance of Pd nanoparticles supported on reduced graphitic oxide nanosheets (Pd/r-GO).[57] They obtained the highest TON (7088) using 1 wt% Pd/r-GO after a long reaction period (32 h) at 100 ˚C under 4 MPa H_2 pressure (entry 26). However, the catalytic efficiency was gradually decreased while increasing the Pd loading (entries 26 and 28), and this was attributed to the large lattice strain of Pd nanoparticles in 1 wt% Pd/r-GO than in 2 and 5 wt% Pd/r-GO.

Very recently, Nguyen *et al.* studied the catalytic performance of PdNi alloy supported on Carbon Nanotube-Graphene (PdNi/CNT-GR) composite for the direct synthesis of formic acid by CO_2 hydrogenation (without any base).[58] To prevent the stacking of GR and the bundling of CNTs, which usually occurs themselves, CNT-GR composite has been utilized as a support to expose the entire surface areas of CNTs and GR for the catalysis. Interestingly, the bimetallic PdNi/CNT-GR (Pd_3Ni_7/CNT-GR; Pd-30 %, Ni-70 %) produced substantial amount of formic acid (1.92 mmol- TON 6.4) at 40 ˚C under 5 MPa total pressure (entry 29). However, a little amount of acetic acid generation was also observed. By comparing with the efficiency of mono-metallic Ni supported on CNT-GR (Ni/CNT-GR) and Pd supported on CNT-GR (Pd/CNT-GR), it was inferred that the synergic effect of Pd-Ni actually responsible for its catalytic activity.

Hao *et al.* hypothesized that the hydroxyl groups on the surface of a support may enhance the adsorption of CO_2 and the catalytic efficiency of a catalyst.[59] To test the hypothesis, ruthenium hydroxide was supported on three different supports; (1) MgO which do not have hydroxyl groups (Ru/MgO); (2) activated carbon which have a limited number of hydroxyl groups on the surface (Ru/AC); and (3) γ-alumina, which have abundant hydroxyl groups on the surface (Ru/γ-Al_2O_3). As they hypothesized, Ru/MgO did not produce formate and Ru/AC showed little activity (TON 10), and Ru/γ-

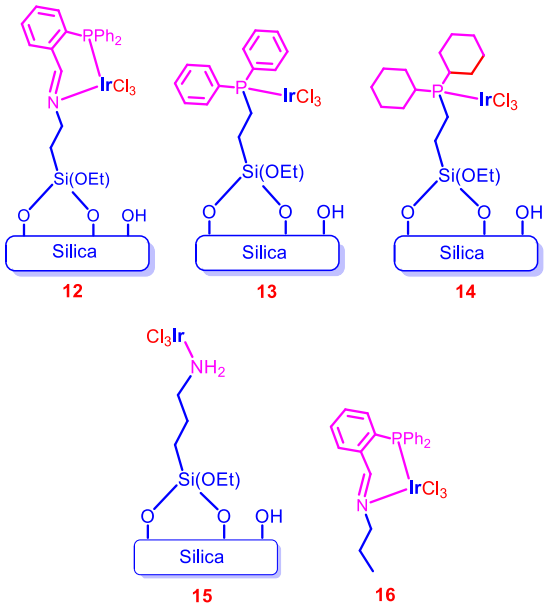

Chart 2. Representative structures of catalysts **12-16**

Al_2O_3 showed higher catalytic activity (TON 91) (entries 30-32). Unlike Pd/AC and Pd/Al_2O_3, Ru/γ-Al_2O_3 exhibited higher catalytic efficiency than Ru/AC. This might be due to the synergic effect of metal and support. Moreover, they observed that presence of RuO_2 on the surface of catalyst (formed during catalyst preparation) lowers the efficiency of the catalyst. Later, Liu *et al.* employed γ-Al_2O_3 nanorods (γ-Al_2O_3(n)) to support the ruthenium hydroxide species (Ru/γ-Al_2O_3(n)) owing to the high surface area, abundant hydroxyl groups, and its increased interaction with ruthenium species.[60-61] As expected, the catalytic efficiency of Ru/γ-Al_2O_3(n) (TON 731) was higher than Ru/γ-Al_2O_3 under similar reaction conditions (entries 32-33).

3. Heterogenized Molecular Catalysts

Heterogeneous metal catalysts demonstrated the possibilities to the separation of catalysts from reaction mixtures and continuous use for repeated runs. However, the catalytic efficiencies of these catalysts were poor; for example, the maximum TOF obtained using these metal-based heterogeneous catalysts was 836 h^{-1} (entry 21).[55] Since these catalysts are mainly made from precious metals (Ru, Pd, Au, etc.), achieving high catalytic efficiency is essential for their economical use. Conversely, homogeneous metal complexes have shown tremendous catalytic efficiencies (TONs up to 3,500,000, [38] TOFs up to 1,100,000 h^{-1}),[40] but are difficult to separate from reaction mixtures. Therefore, much research on the development of heterogeneous catalysts with high catalytic efficiencies has been undertaken. In this context, strategies involving the heterogenization of homogeneous metal complexes have been developed. These strategies seek to develop materials that combine the activity

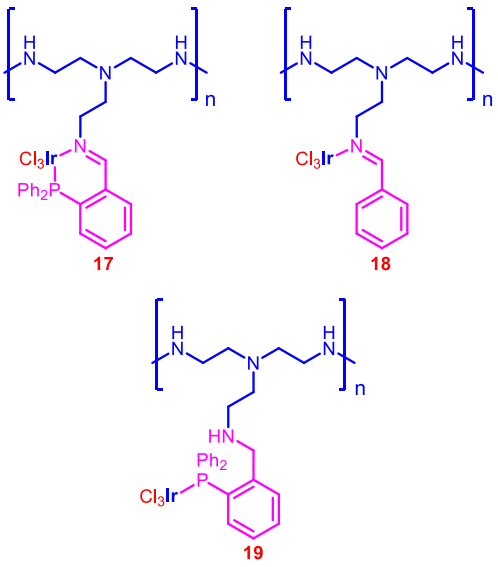

Chart 3. Representative structures of catalysts **17-19**

and selectivity of homogeneous metal catalysts with the advantages of heterogeneous catalysts, i.e., recyclability and easy seclusion from reaction mixtures. Such heterogenization processes, also called 'immobilization', have been performed to produce heterogenized catalysts for CO_2 hydrogenation to formate.

3.1 Grafted Molecular Catalysts

Krocher *et al.* was prepared silica tethered Ru complexes (**1** and **2)** through the covalent bond between the ligand and support for the synthesis of dimethylformamide from CO_2 (Chart 1).[62] Later, Zheng and co-workers immobilized the Ru complexes on the surface of supports through the coordination bond between the donor ligand of the support and the metal ion (Chart 1, **3**-**11**).[63-67] They extensively studied the effect of various supports (silica, MCM-41 and polystyrene (PS)) and surface-bound donor ligands (amine (-NR_2), nitrile (-CN) and thiol (-SH)) for the hydrogenation of CO_2 to formate. To study the effect of supports on reactivity, both inorganic and organic supports have been considered. For the inorganic supports, only silica based supports (silica and MCM-41) were employed which might be due to the ease of functionalization through their surface OH-groups and their rigid structure. Among the inorganic supports, MCM-41 supported catalyst (**3**) showed higher activity than silica supported catalyst (**4**) (entries 34 and 35). The high surface area (852 m^2 g^{-1}) and uniform pores (3.5 nm) of MCM-41 were responsible for this result, indicating that the porous catalysts together with large surface area would be the possible candidates for better catalytic efficiency. Regarding the organic supports, only PS was investigated. The catalytic efficiency of PS supported catalyst (**5**) was found to be very low (TOF-151 h^{-1}) under similar reaction conditions (entries 34 and 36). Considering the amine (**3**), nitrile (**6**) and thiol (**7**) functionalities on the surface of support, the amine functionalized catalyst (**3**) exhibited better activity than **6** and **7** (entries 34, 37 and 38). This might be due to the strong electron donating ability of amine groups to metal ion than those of nitrile and thiol groups. Of the primary (**4**), secondary (**8**) and tertiary amine (**9**) functionalized complexes, the secondary amine functionalized complex (**8**) showed highest TOF (1384 h^{-1}) (entries 35, 39 and 40). This again reveals that the strong electron donating ligands increases the efficiency of the catalyst as secondary amine is better electron donor than primary and tertiary amines. Similar trend was obtained while considering catalysts **5**, **10** and **11** (entries 35, 41 and 42). Conversely, recycling experiments of **3**, **6** and **7** showed that catalysts **3** and **6** deactivated more significantly than catalyst **7**. This may be the better back donating ability of thiol group than the nitrile and amine functional groups; thus, the bond between metal and thiol donor ligand of the support remains stronger.

Furthermore, these Ru complexes produced the formate only in the presence of external ligands/additives (PPh_3, $AsPh_3$, NPh_3 and $Ph_2P(CH_2)_2PPh_2$ (dppe)), suggesting the in situ formed active catalyst contained external ligand as one of the ligands (Chart 1, showed the expected active catalyst (**4A)** for catalyst **4**).[64] They have also studied the outcome of the reaction with various additives and observed that the bidentate ligand, dppe, exhibited higher catalytic efficiency than the monodentate ligands (entry 34, 36, 43-46). This was attributed to the smaller bite angle of the dppe ligand (313.082˚, 313.418˚) than the PPh_3 ligand (314.76˚), which consequently reduces the steric hindrance of dppe ligand with the Ru ion. Therefore, the coordination of dppe with metal ions was more favorable than PPh_3, which led to the higher activity of dppe containing catalysts.[67]

In 2008, Zhang *et al.* employed ionic liquid (IL) as a reusable base to isolate formic acid from formate.[68] In light of Zheng and co-workers results, [63-67] they have employed silica supported Ru complex ["Si"-$(CH_2)_3NH(CSCH_3)$-{$RuCl_3(PPh_3)$}] as a catalyst for this purpose. The catalyst in combination with amine functionalized IL promoted the CO_2 hydrogenation with a maximum TOF of 103 h^{-1}. Almost 1:1 molar ratio of formic acid to IL (used) was observed, indicating the complete consumption of the added IL. They also prepared diamine-functionalized IL to improve the efficiency of CO_2 hydrogenation.[69] The maximum TOF of 920 h^{-1} was obtained at relatively high temperature (80 ˚C) and pressure (18 MPa total pressure). As expected, the molar ratio of formic acid to IL was reached up to 2:1. Notably, the free formic acid was separated from the IL with the aid of N_2 flow at 130 ˚C and the catalyst and IL were reused for several runs. These unique features of this method offer the opportunity to apply the reaction in commercial process.

Hicks and co-workers further functionalized the amine groups of the mesoporous silica into imine groups by Schiff base reaction with o-(diphenylphosphino)benzaldehyde, and immobilized Ir complexes through an imine-phosphine coordination bond (**12**).[70] For comparison, monodentate phosphine complexes (**13** and **14**), amine precatalyst **15** and the homogeneous counterpart (**16**) were synthesized (Chart

2). X-ray photoelectron Spectroscopy (XPS) measurements of **12** and **16** showed that the environment of Ir in **12** (61.6 eV) and **16** (61.8 eV) are similar. Among the catalysts screened (**12**, **13**, **14**, **15** and **16**), only phosphine containing catalysts (**12**, **13**, **14** and **16**) were showed activity in CO_2 hydrogenation to formate (entries 47-50). Catalyst **12** exhibited a higher TON (1300) than **13** (110) and **14** (400) (entries 47-49). Moreover, **12** showed almost 20 times higher efficiency than unsupported catalyst (**16**), revealing the increased stability and activity upon heterogenization of homogeneous complexes (entries 47 and 51). The catalytic efficiency was increased with temperature, and the highest TOF of 1200 h^{-1} was attained at 120 ˚C (entries 52-54). Time-dependent formate production studies showed that formate production increased with time, and the catalyst exhibited the maximum TON (2700) and afforded a maximum concentration of formate (0.270 M) at 60 ˚C after 20 h (entries 47, 52 and 55). Catalyst **12** was recycled at minimum time intervals (0.5 h) under mild conditions and obtained the average TON of 70.

Hicks and co-workers also employed polyethyleneimine (PEI), an aliphatic amine-based organic polymer containing primary, secondary and tertiary amine groups, as a support to immobilize the Ir complexes.[71] It was expected that this amine-based support would be multifunctional, acting as CO_2 capturing material, formate stabilizer and catalyst support. Hence, the catalyst **17** was prepared by tethering complex **16** on this PEI (Chart 3). They compared the activity of **17** with an imine containing catalyst (**18**) and a phosphine containing catalyst (**19**) and found that **17** exhibited better activity than **18** and **19** (entries 56-58). However, it is noteworthy that the efficiency of **17** is poor when compared to **12** (entries 54 and 56), indicating the weakness of PEI supports. Additionally, it was found that varying the amount of Ir loading [Ir-25 % (PEI-PN/Ir-25), Ir-65 % (PEI-PN/Ir-65) and Ir-95 % (PEI-PN/Ir-95)] on the PEI backbone affected the efficiency of catalyst; PEI-PN/Ir-65 exhibited better efficiency (TOF 310 h^{-1}) than PEI-PN/Ir-25 (TOF 94 h^{-1}) and PEI-PN/Ir-95 (TOF 122 h^{-1}). XPS and TEM measurements revealed the existence of agglomerated Ir nanoparticles on the surface of PEI-PN/Ir-25 and PEI-PN/Ir-95, whereas no such agglomerated Ir nanoparticles were observed in PEI-PN/Ir-65. Consequently, they suggested that the Ir nanoparticles are catalytically inactive for the hydrogenation of CO_2 to formate. In addition, the efficiency of catalysts was also affected by the PEI molecular weight (PEI-MW). Moreover, recycling experiments demonstrated that the efficiency of catalysts decreases continuously, especially for low PEI-MW catalyst, owing to the increased solubility and formation of inactive Ir species. Furthermore, the catalysts exhibited poor activity in the absence of external base, suggesting that the amines present in the backbone of PEI no longer significantly stabilize the formate under these conditions.

3.2 Heterogenized COF Catalysts

Since the Ir/Ru complexes heterogenized on conventional silica, PS and aliphatic polymer supports demonstrated low catalytic activity and stability,[63-71] the research on new strategies/supports to immobilize the homogeneous complexes are inevitable. Thus, porous organic polymers have been used as catalyst supports owing to their high surface area, well-defined porosity, ease of use and the diverse number of synthetic routes.[72] Specifically, crystalline microporous organic polymers with ordered porous

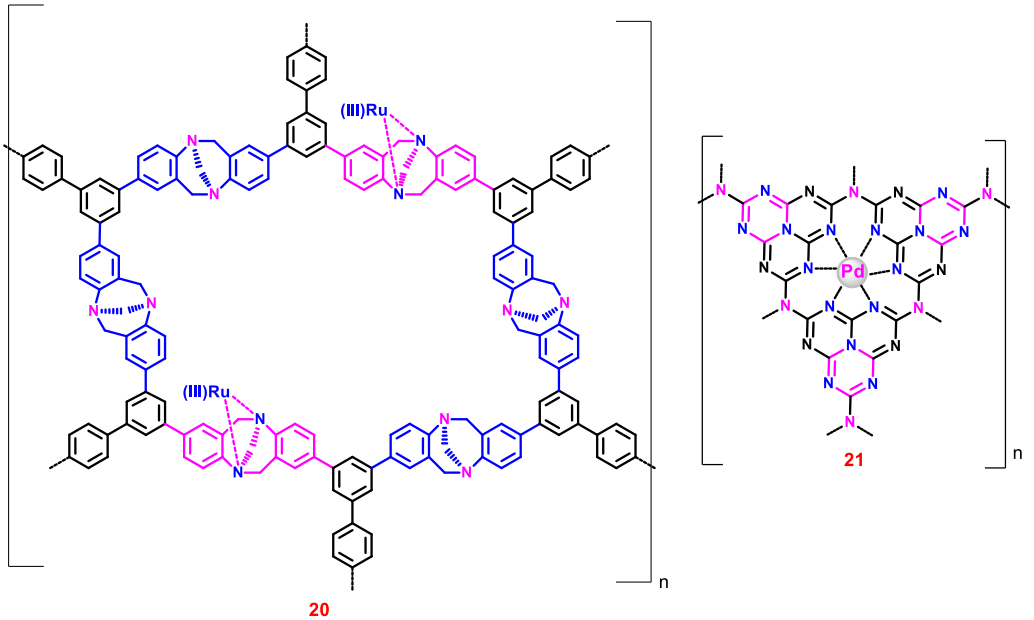

Chart 4. Structural representation of catalysts **20** and **21**

structures – so called 'covalent organic frameworks' (COFs) – have drawn particular attention due to their low density, high thermal stability, large surface area, tunable pore size and structure, and versatile covalent combination of building blocks.[73] These polymeric materials have used as gas storage materials, catalyst supports and photonic band gap materials.[74-78] Consequently, COFs like Troger's base-derived microporous organic polymers (TB-MOPs),[79] graphitic carbon nitrides (g-C_3N_4),[80] triazine-based covalent organic frameworks (CTFs)[81] and heptazine-based covalent organic frameworks (HBFs)[82] have been employed as catalyst supports for CO_2 hydrogenation to formate.

Liu and co-workers prepared a TB-MOP supported Ru(III) catalyst (**20**) through the coordination bond between the N atoms of the TB-MOP and the Ru(III) ions (Chart 4).[79] The microporous structure of **20** was confirmed by Brunauer-Emmett-Teller (BET) measurements. The catalyst **20** exhibited the substantial catalytic efficiency (TON-2254) in the presence of PPh_3 ligands at 40 ˚C under 12 MPa total pressure (entry 60). However, in the absence of PPh_3 ligands the TON was decreased to 25 (entries 59 and 60), suggesting the active catalyst was formed *in situ*, and that the structure of active catalyst could be similar to that proposed by Zheng and co-workers[64].

Later, Lee *et al.* demonstrated the catalytic performance of Pd nanoparticles supported on mesoporous g-C_3N_4 (**21**) (Chart 4).[80] The TON for **21** in 20 % NEt_3-Deuterium oxide (D_2O) solution was found to be 81 at 150 ˚C under $p(H_2)/p(CO_2)$ =1 (entry 61). Interestingly, the relative ratio of gas pressures [$p(H_2)/p(CO_2)$] affected the outcome of the reaction; TON was increased to 106 at $p(H_2)/p(CO_2)$ = 2 (entries 61 and 62). However, TON was reduced on increasing the ratio further (entries 62 and 64).

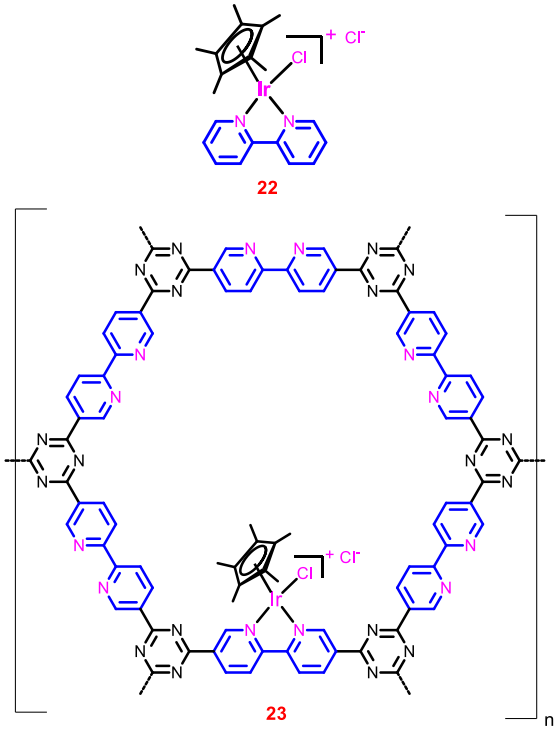

Chart 5. Structural representation of catalysts **22** and **23**

Over the past ten years, homogeneous [IrCp*(N-N)X]Y complexes (N-N represents bipyridine (bpy), phenonthroline and pyrimidine derivatives, Cp*-1,2,3,4,5-pentamethyl cyclopentadiene, X-Cl/H_2O, Y-Cl/SO_4^{2-}) have shown tremendous catalytic activities and selectivities.[83-85] The highest TON (222,000) and maximum TOF (53,800 h^{-1}) were obtained with these catalysts by Himeda *et al.*[35,83] Since these catalysts are proton-responsive and pH-switchable, their catalytic activity and H_2O solubility can be tuned by pH of the solution. Thus, at the end of the CO_2 hydrogenation (a decrease in the pH of the solution leaded by reaction equilibrium), the catalyst can be precipitated because of its low solubility in weak acidic solution (pH 5.5).[86] However, this unique property is only observed for the Ir-phenonthroline derivative. Recently, Yoon and co-workers developed a new strategy to heterogenize the homogeneous [IrCp*(bpy)Cl]Cl complex (**22**) (Chart 5).[81] They employed a bpy incorporated CTF (bpy-CTF) as a support owing to its high thermal stability, large pore volumes and high surface areas. The bpy-CTF has the potential to form complexes with metal precursors (Chart 5). They hypothesized that the complex resulting from the reaction of $[IrCp^*Cl_2]_2$ and bpy-CTF would have a similar coordination environment as that of complex **22**. As they hypothesized, the heterogenized complex, bpy-CTF-[IrCp*Cl]Cl (**23**), was synthesized and thoroughly characterized to prove its exact coordination environment as that of complex **22**. Scanning electron microscopy (SEM) measurements of **23** illustrated the uniform distribution of Ir and Cl atoms throughout the complex, suggesting the uniform metalation of Ir ions onto bpy moieties. In addition, Energy dispersive X-ray spectroscopy (EDS) as well as XPS measurements revealed that the atomic ratio of Ir and Cl was close to 1:2. Moreover, XPS measurements of both **22** and **23** showed that they have exactly same EBE value for Ir $4f_{7/2}$ (62.1 eV), reiterating the similar coordination environment of Ir in both the catalysts. Inductively coupled plasma mass spectrometry (ICP-MS) analysis of **23** showed that it has relatively high Ir content (4.7 wt%) in the framework, indicating every sixth CTF ring unit contains one {IrCp*} unit.

The temperature-dependent catalytic performance of **23** showed that the activity increased with temperature up to 120 ˚C, thereafter decreased as the temperature increased further (entries 65 and 68). This is attributed to the exothermic nature of the reaction. However, the catalytic activity increased with pressure and attained a maximum TON of 5,000 at 120 ˚C under 8 MPa total pressure (entry 69). The time-dependent formate generation studies revealed that the reaction attained equilibrium (0.6-0.7 M formate concentration) within a relatively short reaction time (2 h). In addition, under relatively mild conditions, catalyst **23** showed the highest ever initial TOF of 5,300 h^{-1} for the conversion of CO_2 to formate using heterogeneous catalysts (entry 70). Moreover, catalyst **23** was recycled over five runs without

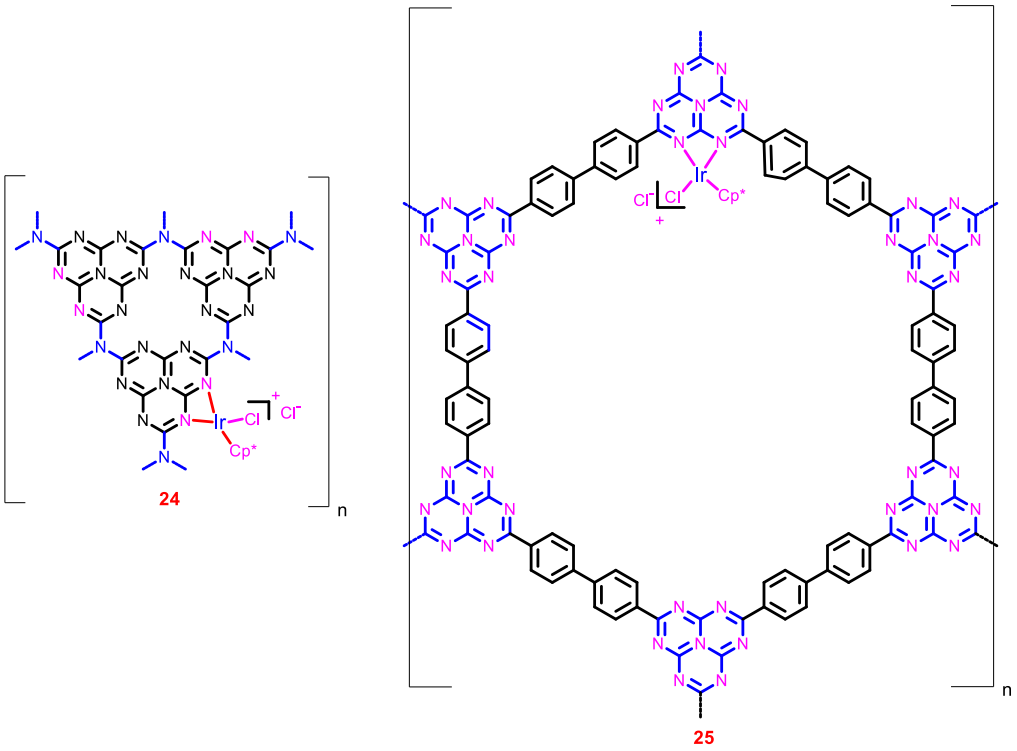

Chart 6. Structural representation of catalysts **24** and **25**

significant loss of activity and on each recycling ca. 92 % catalytic activity was maintained.

Vey recently, Yoon and co-workers have also heterogenized the [IrCp*(N-N)X]Y complex using g-C_3N_4 (**24**) and HBF (**25**) supports (Chart 6).[82] The uniform metalation as well as the ratio of Ir to Cl (1:2) were confirmed by SEM and EDS measurements, respectively. ICP-MS analysis of **25** showed very less Ir content (0.86 wt%) in the framework. The catalyst **25** exhibited an initial TOF of 1500 h^{-1} and TON of 6400 at 120 ˚C under 8 MPa total pressure (entries 71 and 72). The catalyst was recycled without significant loss of activity and stability, and on each recycling ca. 90 % catalytic activity was maintained with an average TON of 4000.

4. Theoretical Investigations

Even though the research on development of efficient catalyst is progressive, understanding the complete reaction mechanism through the experimental research is rather difficult and time consuming. This is due to the fact that finding substrate-catalyst interactions, energies of molecules involved, transition states and intermediates structure, and activation barriers for the process is quite difficult.[87] To overcome these limitations, theoretical calculations have become powerful tools to investigate the reaction pathway.[88] Moreover, the key structure-activity relationship for the rational design of suitable and efficient catalyst could be gained through this study.

Synthesis of formic acid and methanol from CO_2 and H_2 involves formate as one of the intermediate. Hence, many reports discussed the reaction pathway for the formation of formic acid, free formate anion and catalyst bound formate from CO_2 and H_2.[89-91] However, the calculations involving only formic acid formation using heterogeneous catalysts are presented in here.[92-97]

Peng *et al.* theoretically explored CO_2 hydrogenation to formic acid on Ni(111) surfaces.[92] They investigated the reaction mechanism via two routes, namely formate intermediate route (HCOO**) in which CO_2 can be hydrogenated at its carbon atom and carboxyl intermediate route (COOH*) in which CO_2 can be hydrogenated at its oxygen atom, using Ni(111) surfaces. Their calculations showed that for the formation of HCOO** a lower activation energy (14.3 kcal mol^{-1}) is required than for the COOH* (19.1 kcal mol^{-1}). This result clearly suggests that the HCOO** route is more favorable than COOH* route. Previously, Vesselli *et al.* concluded that the COOH* route preferably produce CO and H_2O instead of formic acid by Ni(110) surface. [93] Peng *et al.* also studied the second hydrogenation step, that is the formation of formic acid from HCOO**, and found that it has very high activation barrier (14.3 kcal mol^{-1}), suggesting this might be the rate-determining step for formic acid production.[92] Overall, the reaction is highly endothermic (12.9 kcal mol^{-1}). Moreover, they also extensively studied to reduce such a high activation barrier and concluded that if subsurface H [absorbed in the subsurface of Ni(111)] involve in the second hydrogenation step, the activation barrier could be lowered and can make the overall reaction exothermic (-16.3 kcal mol^{-1}). Similar results were obtained for Ni(110) surfaces.[94]

Limtrakul and co-workers theoretically investigated the reaction mechanism of hydrogenation of CO_2 to formic acid catalyzed by Cu-alkoxide-functionalized metal organic framework (Cu-MOF-5).[95] Two different reaction pathways

are proposed, namely concerted and stepwise mechanisms. In both the pathways, reactants (CO_2 and H_2) are initially adsorbed on the Cu-MOF-5 catalyst and form the coadsorption complex. For the concerted mechanism, the reaction is proposed to take place in a single step with the active site of catalyst not assisting the H_2 splitting. In the transition state of this pathway, the adsorbed CO_2 is simultaneously hydrogenated at the C and O atom to form formic acid. The activation barrier for this pathway is calculated to be 67.2 kcal mol^{-1}. For the stepwise mechanism, in which a part of the active site assists the H_2 splitting, the reaction occurs via two steps involving a formate intermediate. The first step, which is the formation formate intermediate, is found to be the rate-determining step with the activation energy of 24.2 kcal mol^{-1}. The more facile second step, in which the proton is transferred to the formate intermediate, has a smaller activation barrier (18.3 kcal mol^{-1}). Because of the smaller activation barriers associated with this pathway (24.2 vs 67.2 kcal mol^{-1}), it, therefore, seems to be more favored over the concerted one. Furthermore, the catalytic effect of Cu-MOF-5 is also compared with the gas-phase uncatalyzed reaction in which the reaction takes place in one step with a barrier of 73.0 kcal mol^{-1}. Therefore, this investigation clearly infers the two important design strategies for efficient catalysts for this reaction. (1). the catalysts would adsorb the reactants. (2). it would assist the H_2 splitting.

Since the frustrated Lewis pairs (FLPs) are capable of activating CO_2 and heterolytically dissociating H_2, Ye *et al.* theoretically demonstrated the reaction mechanism of hydrogenation of CO_2 to formic acid catalyzed by Lewis pair-functionalized metal organic framework (UiO-66-P-BF_2).[96] They investigated the reaction in two different approaches. In the first approach, H_2 is activated initially by dissociative adsorption, and then reacting with physisorbed CO_2 to produce formic acid. In this pathway, the addition of hydridic and protic hydrogens (chemisorbed H atoms) to C and O of physisorbed CO_2 respectively, occurs in a concerted fashion with the activation barrier of 10.8 kcal mol^{-1}. In the second approach, CO_2 is activated initially by chemisorptions, and then reacting with physisorbed H_2. However, in this approach, the undesired formyl and hydroxyl moieties were produced with high activation barrier rather than the desired formic acid product. This is because the CO_2 bound too strongly with the FLP of UiO-66-P-BF_2 through chemisorption. Hence, for the UiO-66-P-BF_2 catalyst to work in practice, one would have to expose the material first to H_2 and then to CO_2 to avoid the competing reaction and potential poisoning of the catalyst. This requirement would prohibit its practical use. Therefore, the designed catalyst should weakly bind with CO_2 through FLP (P-BF_2) and at the same time it would provide a binding site that selectively dissociates H_2.

Limtrakul and co-workers also explored the catalytic reaction pathway of Cu embedded in the surface of graphene (Cu/dG) for the CO_2 hydrogenation to formic acid.[97] Initially, they studied the properties of Cu/dG through their calculations and found that the catalyst Cu/dG binds more strongly with H_2 (adsorption energy = -6.12 kcal mol^{-1}) than CO_2 (adsorption energy = -5.1 kcal mol^{-1}). In addition, the Cu/dG is more selective for the adsorption of H_2 molecule rather than the CO_2 molecule. They investigated the course of the reaction via two paths. In the first path, the reaction takes place in two steps. In the initial step, the first hydrogenation of CO_2 takes place, without activating the H_2 molecule, through the highest activation barrier (34.6 kcal mol^{-1}) and produces the unstable H-Cu-COOH intermediate. In the later step, the second hydrogenation takes place through the H-transfer from the Cu atom to the carbon of the –COOH moiety via three membered ring with the activation barrier of 4.0 kcal mol^{-1}. Finally, formic acid is released from the Cu/dG catalyst with the activation energy of 20.1 kcal mol^{-1}. For the second route, the H_2 molecule is activated by dissociating H_2 molecule to Cu-H and C-H (from grapheme carbon) moieties in the first step with the highest energy barrier of 19.7 kcal mol^{-1}. In the second step, the insertion of CO_2 into the Cu-H species to form the formate intermediate (HCOO-Cu/H-dG) is much more favorable (-14.6 kcal mol^{-1}) and requires the activation energy of 13.6 kcal mol^{-1}. Finally, the protonation of formate intermediate preferably takes place with the second H_2 molecule (11.6 kcal mol^{-1}). Therefore this study infers that the H_2 activated route would be more facile than the inactivated H_2 route.

5. Summary and Conclusions

Diverse forms of heterogeneous catalysts for the conversion of CO_2 into formate have evolved to meet the requirements for industrial application. The following features have emerged as being important for achieving this challenging goal. The heterogeneous catalyst should be sufficiently active to generate enough formate within relatively short period of reaction time. Catalyst's support framework should be sufficiently robust to prevent deleterious decomposition of catalytic active site in harsh reaction condition (pH = 13). The catalysts should be easily separated from reaction mixture at the end of reaction and recycled. Most of these requirements are fulfilled by heterogenization of homogeneous Ir complexes by incorporating onto the pore of the covalent organic frameworks.

Although the field has gone through a rapid progression phase, more work must be carried out to achieve remaining important goals of the development of catalysts for the conversion of CO_2 into formate. The first is to obtain a system having the extreme stability over repeated recycle. Another is to generate the catalyst with cheap transition metal ion(s).

Acknowledgements

We acknowledged the financial support through grants from Korea CCS R&D Center, funded by the Ministry of Education, Science and Technology of Korean government and also from Global Scholarship Program for Foreign Graduate Students at Kookmin Universtiy in Korea.

References

1 H. Arakawa, M. Aresta, J. N. Armor, M. A. Barteau, E. J. Beckman, A. T. Bell, J. E. Bercaw, C. Creutz, E. Dinjus, D. A. Dixon, K. Domen, D. L. DuBois, J. Eckert, E. Fujita, D. H. Gibson, W. A. Goddard, D. W. Goodman, J. Keller, G. J. Kubas, H. H. Kung, J. E. Lyons, L. E. Manzer, T. J. Marks, K. Morokuma, K. M. Nicholas, R. Periana, L. Que, J. Rostrup-Nielson, W. M. Sachtler, L. D. Schmidt, A. Sen, G. A. Somorjai, P. C. Stair, B. R. Stults and W. Tumas, *Chem. Rev.*, 2001, **101**, 953-996.

2 M. Aresta, A. Dibenedetto and A. Angelini, *Chem. Rev.*, 2014, **114**, 1709-1742.

3 A. M. Appel, J. E. Bercaw, A. B. Bocarsly, H. Dobbek, D. L. DuBois, M. Dupuis, J. G. Ferry, E. Fujita, R. Hille, P. J. Kenis, C. A. Kerfeld, R. H. Morris, C. H. Peden, A. R. Portis, S. W. Ragsdale, T. B. Rauchfuss, J. N. Reek, L. C. Seefeldt, R. K. Thauer and G. L. Waldrop, *Chem. Rev.*, 2013, **113**, 6621-6658.

4 S. N. Riduan and Y. Zhang, *Dalton Trans.*, 2010, **39**, 3347-3357.

5 D. J. Darensbourg and S. J. Wilson, *Green Chem.*, 2012, **14**, 2665-2671.

6 C. Maeda, Y. Miyazaki and T. Ema, *Catal. Sci. Technol.*, 2014, **4**, 1482-1497.

7 http://www.nature.com/news/lima-talks-map-out-path-to-climate-treaty-1.16557 (accessed on 2016.01.06)

8 https://unfccc.int/files/meetings/lima_dec_2014/application/pdf/auv_cop20_lima_call_for_climate_action.pdf (accessed on 2016.01.06)

9 G. Ferey, C. Serre, T. Devic, G. Maurin, H. Jobic, P. L. Llewellyn, G. De Weireld, A. Vimont, M. Daturi and J. S. Chang, *Chem. Soc. Rev.*, 2011, **40**, 550-562.

10 D. Sivanesan, Y. Choi, J. Lee, M. H. Youn, K. T. Park, A. N. Grace, H.-J. Kim and S. K. Jeong, *ChemSusChem*, 2015, **8**, 3977-3982.

11 M. Mikkelsen, M. Jorgensen and F. C. Krebs, *Energy Environ. Sci.*, 2010, **3**, 43-81.

12 P. Sudakar, D. Sivanesan and S. Yoon, *Macromol. Rapid Commun*., DOI: 10.1002/marc.201500681.

13 D. J. Darensbourg and M. W. Holtcamp, *Coord. Chem. Rev.*, 1996, **153**, 155-174.

14 T. Sakakura, J. C. Choi and H. Yasuda, *Chem. Rev.*, 2007, **107**, 2365-2387.

15 M. R. Kember, A. Buchard and C. K. Williams, *Chem. Commun.*, 2011, **47**, 141-163.

16 M. Peters, B. Kohler, W. Kuckshinrichs, W. Leitner, P. Markewitz and T. E. Muller, *ChemSusChem*, 2011, **4**, 1216-1240.

17 E. A. Quadrelli, G. Centi, J.-L. Duplan and S. Perathoner, *ChemSusChem*, 2011, **4**, 1194-1215.

18 A. Baiker, *Appl. Organomet. Chem.*, 2000, **14**, 751-762.

19 W. Reutemann and H. Kieczka, Formic acid, Ullmann's Encyclopedia of Industrial Chemistry, Wiley-VCH, Weinheim, 2011.

20 M. Grasemann and G. Laurenczy, *Energy Environ. Sci.*, 2012, **5**, 8171-8181.

21 H.-L. Jiang, S. K. Singh, J.-M. Yan, X.-B. Zhang and Q. Xu, *ChemSusChem*, 2010, **3**, 541-549.

22 S. Uhm, H. J. Lee and J. Lee, *Phys. Chem. Chem. Phys*., 2009, **11**, 9326–9336.

23 S. Moret, P. J. Dyson and G. Laurenczy, *Nat. Commun.*, 2014, **5**, 4017.

24 N. von der Assen, P. Voll, M. Peters and A. Bardow, *Chem. Soc. Rev.*, 2014, **43**, 7982-7994.

25 P. G. Jessop, T. Ikariya and R. Noyori, *Chem. Rev.*, 1995, **95**, 259-272.

26 Y. Inoue, H. Izumida, Y. Sasaki and H. Hashimoto, *Chem. Lett.*, 1976, 863-864.

27 P. G. Jessop, Y. Hsiao, T. Ikariya and R. Noyori, *J. Am. Chem. Soc.*, 1996, **118**, 344-355.

28 F. Joo, G. Laurenczy, L. Nadasdi and J. Elek, *Chem. Commun.*, 1999, 971-972.

29 P. G. Jessop, F. Joo and C. C. Tai, *Coord. Chem. Rev.*, 2004, **248**, 2425-2442.

30 C. Ziebart, C. Federsel, P. Anbarasan, R. Jackstell, W. Baumann, A. Spannenberg and M. Beller, *J. Am. Chem. Soc.*, 2012, **134**, 20701-20704.

31 M. S. Jeletic, M. T. Mock, A. M. Appel and J. C. Linehan, *J. Am. Chem. Soc.*, 2013, **135**, 11533-11536.

32 Y. M. Badiei, W.-H. Wang, J. T. Hull, D. J. Szalda, J. T. Muckerman, Y. Himeda and E. Fujita, *Inorg. Chem.*, 2013, **52**, 12576-12586.

33 Y. Himeda, N. Onozawa-Komatsuzaki, H. Sugihara and K. Kasuga, *J. Photochem. Photobiol., A*, 2006, **182**, 306-309.

34 Y. Himeda, *Eur. J. Inorg. Chem.*, 2007, 3927-3941.

35 J.F. Hull, Y. Himeda, W.-H. Wang, B. Hashiguchi, R. Periana, D.J. Szalda, J.T. Muckerman and E. Fujita, *Nat. Chem.*, 2012, **4**, 383-388.

36 E. Fujita, J. T. Muckerman and Y. Himeda, *Biochim. Biophys. Acta*, 2013, **1827**, 1031-1038.

37 S. Sanz, M. Benitez and E. Peris, *Organometallics*, 2010, **29**, 275-277.

38 R. Tanaka, M. Yamashita and K. Nozaki, *J. Am. Chem. Soc.*, 2009, **131**, 14168-14169.

39 G. A. Filonenko, E. J. M. Hensen and E. A. Pidko, *Catal. Sci. Technol.*, 2014, **4**, 3474-3485.

40 G. A. Filonenko, R. van Putten, E. N. Schulpen, E. J. M. Hensen and E. A. Pidko, *ChemCatChem*, 2014, **6**, 1526-1530.

41 D. Preti, S. Squarcialupi and G. Fachinetti, *Angew. Chem. Int. Ed.*, 2010, **49**, 2581-2584.

42 C. Fellay, P. J. Dyson and G. Laurenczy, *Angew. Chem. Int. Ed.*, 2008, **47**, 3966-3968.

43 T. Schaub and R. A. Paciello, *Angew. Chem. Int. Ed.*, 2011, **50**, 7278-7282.

44 W. Wang, S. Wang, X. Ma and J. Gong, *Chem. Soc. Rev.*, 2011, **40**, 3703-3727.

45 S. Saeidi, N. A. S. Amin and M. R. Rahimpour, *J. CO_2 Util.*, 2014, **5**, 66-81.

46 A. Behr and K. Nowakowski, *Adv. Inorg. Chem.*, 2014, **66**, 223-258.

47 W.-H. Wang, Y. Himeda, J. T. Muckerman, G. F. Manbeck and E. Fujita, *Chem. Rev.*, 2015, **115**, 12936-12973.

48 M. W. Farlow and H. Adkins, *J. Am. Chem. Soc.*, 1935, **57**, 2222-2223.

49 C. J. Stalder, S. Chao, D. P. Summers and M. S. Wrighton, *J. Am. Chem. Soc.*, 1983, **105**, 6318-6320.

50 H. Takahashi, L. H. Liu, Y. Yashiro, K. Ioku, G. Bignall, N. Yamasaki and T. Kori, *J. Mater. Sci.*, 2006, **41**, 1585-1589.

51 D. Preti, C. Resta, S. Squarcialupi and G. Fachinetti, *Angew. Chem. Int. Ed.*, 2011, **50**, 12551-12554.

52 http://authors.library.caltech.edu/25070/6/FundChemReaxEngCh5.pdf (accessed on 2016.01.06)

53 D. Preti, S. Squarcialupi and G. Fachinetti, *ChemCatChem*, 2012, **4**, 469-471.

54 G. A. Filonenko, W. L. Vrijburg, E. J. M. Hensen and E. A. Pidko, *J. Catal.*, DOI: 10.1016/j.jcat.2015.10.002.

55 J. Su, L. Yang, M. Lu and H. Lin, *ChemSusChem*, 2015, **8**, 813-816.

56 J. Su, M. Lu and H. Lin, *Green Chem.*, 2015, **17**, 2769-2773.

57 Q.-Y. Bi, J.-D. Lin, Y.-M. Liu, D.-L. Du, J.-Q. Wang, H.-Y. He and Y. Cao, *Angew. Chem. Int. Ed.*, 2014, **53**, 13583-13587.

58 L. T. M. Nguyen, H. Park, M. Banu, J. Y. Kim, D. H. Youn, G. Magesh, W. Y. Kim and J. S. Lee, *RSC Adv*., 2015, **5**, 105560-105566.

59 C. Y. Hao, S. P. Wang, M. S. Li, L. Q. Kang and X. Ma, *Catal. Today*, 2011, **160**, 184-190.
60 N. Liu, R. Du and W. Li, *Adv. Mater. Res.*, 2013, **821-822**, 1330-1335.
61 N. Liu, J. Lei, M. Li and P. Wang, *Adv. Mater. Res.*, 2014, **881-883**, 283-286.
62 O. Krocher, R. A. Koppel, M. Froba and A. Baiker, *J. Catal.*, 1998, **178**, 284-298.
63 Y. Zhang, J. Fei, Y. Yu and X. Zheng, *Catal. Commun.*, 2004, **5**, 643-646.
64 Y. M. Yu, Y. P. Zhang, J. H. Fei and X. M. Zheng, *Chin. J. Chem.*, 2005, **23**, 977-982.
65 Y. M. Yu, J. H. Fei, Y. P. Zhang and X. M. Zheng, *Chin. Chem. Lett.*, 2006, **17**, 1097-1100.
66 Y. M. Yu, J. H. Fei, Y. P. Zhang and X. M. Zheng, *Chin. J. Chem.*, 2006, **24**, 840-844.
67 Y. P. Zhang, J. H. Fei, Y. M. Yu and X. M. Zheng, *Chin. Chem. Lett.*, 2006, **17**, 261-264.
68 Z. Zhang, Y. Xie, W. Li, S. Hu, J. Song, T. Jiang and B. Han, *Angew. Chem. Int. Ed.*, 2008, **47**, 1127-1129.
69 Z. Zhang, S. Hu, J. Song, W. Li, G.Yang and B. Han, *ChemSusChem*, 2009, **2**, 234-238.
70 Z. Xu, N. D. McNamara, G. T. Neumann, W. F. Schneider and J. C. Hicks, *ChemCatChem*, 2013, **5**, 1769-1771.
71 N. D. McNamara and J. C. Hicks, *ChemSusChem*, 2014, **7**, 1114-1124.
72 X. Feng, X. S. Ding and D. L. Jiang, *Chem. Soc. Rev.*, 2012, **41**, 6010-6022.
73 A. Nagai, Z. Q. Guo, X. Feng, S. B. Jin, X. Chen, X. S. Ding and D. L. Jiang, *Nat. Commun.*, 2011, **2**, 536.
74 C. J. Doonan, D. J. Tranchemontagne, T. G. Glover, J. R. Hunt and O. M. Yaghi, *Nat. Chem.*, 2010, **2**, 235-238.
75 J. Roeser, K. Kailasam and A. Thomas, *ChemSusChem*, 2012, **5**, 1793-1799.
76 X. Zhu, C. Tian, S. M. Mahurin, S. H. Chai, C. Wang, S. Brown, G. M. Veith, H. Luo, H. Liu and S. Dai, *J. Am. Chem. Soc.*, 2012, **134**, 10478-10484.
77 L. Hao, J. Ning, B. Luo, B. Wang, Y. Zhang, Z. Tang, J. Yang, A. Thomas and L. Zhi, *J. Am. Chem. Soc.*, 2015, **137**, 219-225.
78 A. Thomas, *Angew. Chem. Int. Ed.*, 2010, **49**, 8328-8344.
79 Z. Yang, H.Zhang, B. Yu, Y. Zhao, G. Ji and Z. Liu, *Chem. Commun.*, 2015, **51**, 1271-1274.
80 J. H. Lee, J. Ryu, J. Y. Kim, S. W. Nam, J. H. Han, T. H. Lim, S. Gautam, K. H. Chae and C. W. Yoon, *J. Mater. Chem. A*, 2014, **2**, 9490-9495.
81 K. Park, G. H. Gunasekar, N. Prakash, K. D. Jung and S. Yoon, *ChemSusChem*, 2015, **8**, 3410-3413.
82 G. Gunniya Hariyanandam, D. Hyun, P. Natarajan, K. D. Jung and S. Yoon, *Catal. Today*, DOI: 10.1016/j.cattod.2015.10.037.
83 Y. Himeda, N. Onozawa-Komatsuzaki, H. Sugihara, H. Arakawa and K. Kasuga, *Organometallics*, 2004, **23**, 1480-1483.
84 W.-H. Wang, J. F. Hull, J. T. Muckerman, E. Fujita and Y. Himeda, *Energy Environ. Sci., 2012, **5**, 7923-7926*.
85 Y. Himeda, N. Onozawa-Komatsuzaki, H. Sugihara and K. Kasuga, *Organometallics*, 2007, **26**, 702-712.
86 Y. Himeda, N. Onozawa-Komatsuzaki, H. Sugihara and K. Kasuga, *J. Am. Chem. Soc.*, 2005, **127**, 13118-13119.
87 J. K. Norskov, T. Bligaard and J. Kleis, *Science*, 2009, **324**, 1655-1656.
88 J. K. Norskov, T. Bligaard, J. Rossmeisl and C. H. Christensen, *Nat. Chem.,* 2009, **1**, 37-46.
89 R. Zhang, B. Wang, H. Liu and L. Ling, *J. Phys. Chem. C*, 2011, **115**, 19811-19818.
90 D. Cheng, F. R. Negreiros, E. Apra and A. Fortunelli, *ChemSusChem*, 2013, **6**, 944-965.
91 Y. Li, S. H. Chan and Q. Sun, *Nanoscale*, 2015, **7**, 8663-8683.
92 G. Peng, S. J. Sibener, G. C. Schatz, S. T. Ceyer and M. Mavrikakis, *J. Phys. Chem. C*, 2012, **116**, 3001-3006.
93 E. Vesselli, M. Rizzi, L. De Rogatis, X. Ding, A. Baraldi, G. Comelli, L. Savio, L. Vattuone, M. Rocca, P. Fornasiero, A. Baldereschi and M. Peressi, *J. Phys. Chem. Lett.*, 2009, **1**, 402-406.
94 G. Peng, S. J. Sibener, G. C. Schatz and M. Mavrikakis, *Surf. Sci.*, 2012, **606**, 1050-1055.
95 T. Maihom, S. Wannakao, B. Boekfa and J. Limtrakul, *J. Phys. Chem. C*, 2013, **117**, 17650-17658.
96 J. Ye and J. K. Johnson, *ACS Catal.*, 2015, **5**, 2921-2928.
97 J. Sirijaraensre and J. Limtrakul, *Appl. Surf. Sci.*, 2016, **364**, 241-248.